

# Alternatively spliced vascular endothelial growth factor receptor-2 is an essential endogenous inhibitor of lymphatic vessel growth

Romulo J C Albuquerque<sup>1,2</sup>, Takahiko Hayashi<sup>3,14</sup>, Won Gil Cho<sup>1,14</sup>, Mark E Kleinman<sup>1,14</sup>, Sami Dridi<sup>1</sup>, Atsunobu Takeda<sup>1</sup>, Judit Z Baffi<sup>1</sup>, Kiyoshi Yamada<sup>1</sup>, Hiroki Kaneko<sup>1</sup>, Martha G Green<sup>1</sup>, Joe Chappell<sup>4</sup>, Jörg Wilting<sup>5</sup>, Herbert A Weich<sup>6</sup>, Satoru Yamagami<sup>7</sup>, Shiro Amano<sup>7</sup>, Nobuhisa Mizuki<sup>3</sup>, Jonathan S Alexander<sup>8</sup>, Martha L Peterson<sup>9</sup>, Rolf A Brekken<sup>10</sup>, Masanori Hirashima<sup>11</sup>, Seema Capoor<sup>1</sup>, Tomohiko Usui<sup>7</sup>, Balamurali K Ambati<sup>12,13</sup> & Jayakrishna Ambati<sup>1,2</sup>

Disruption of the precise balance of positive and negative molecular regulators of blood and lymphatic vessel growth can lead to myriad diseases. Although dozens of natural inhibitors of hemangiogenesis have been identified, an endogenous selective inhibitor of lymphatic vessel growth has not to our knowledge been previously described. We report the existence of a splice variant of the gene encoding vascular endothelial growth factor receptor-2 (Vegfr-2) that encodes a secreted form of the protein, designated soluble Vegfr-2 (sVegfr-2), that inhibits developmental and reparative lymphangiogenesis by blocking Vegf-c function. Tissue-specific loss of sVegfr-2 in mice induced, at birth, spontaneous lymphatic invasion of the normally alymphatic cornea and hyperplasia of skin lymphatics without affecting blood vasculature. Administration of sVegfr-2 inhibited lymphangiogenesis but not hemangiogenesis induced by corneal suture injury or transplantation, enhanced corneal allograft survival and suppressed lymphangioma cellular proliferation. Naturally occurring sVegfr-2 thus acts as a molecular uncoupler of blood and lymphatic vessels; modulation of sVegfr-2 might have therapeutic effects in treating lymphatic vascular malformations, transplantation rejection and, potentially, tumor lymphangiogenesis and lymphedema.

The blood and lymphatic vessel networks are jointly essential for development, wound healing and immune surveillance and activation. Pathological responses of these parallel circulatory systems can lead to diseases as varied as age-related macular degeneration, atherosclerosis, cancer, lymphedema, rheumatoid arthritis and tumor metastasis<sup>1</sup>. Collectively, exuberant or inadequate responses of hemangiogenesis and lymphangiogenesis are estimated to affect nearly two billion people worldwide<sup>2,3</sup>. The prevalence of such diseases has fueled intense efforts to develop pro- and antiangiogenic therapeutics. Several antiangiogenic drugs are US Food and Drug Administration–approved, but, to our knowledge, no lymphangiogenesis-specific inhibitor has yet entered clinical trials. As such, there is great interest in identifying such specific inhibitors both to alleviate disease burden and to better understand lymphatic vascular biology. However, it has been challenging to develop selective approaches

toward modulating lymphangiogenesis due to the difficulty in mechanistically disassociating it from hemangiogenesis.

The Vegf family of molecules is indispensable for growth of blood<sup>4,5</sup> and lymphatic<sup>6</sup> vessels. Hemangiogenesis is governed by a precise balance of positive and negative regulators<sup>7</sup>; however, the mechanisms governing lymphangiogenesis remain nebulous. Soluble VEGFR-1 proteins generated by splice variants in the gene encoding VEGFR-1 act as potent natural inhibitors of hemangiogenesis by trapping the blood endothelial mitogen VEGF-A<sup>8–10</sup>. To our knowledge, other secreted forms of VEGF tyrosine kinase receptors resulting from splice variants have not been previously reported. Here we describe the detection and function of a new secreted VEGF receptor generated by alternative splicing, which we show is an endogenous antagonist of VEGF-C and a crucial regulator of lymphatic vessel growth.

<sup>1</sup>Departments of Ophthalmology & Visual Sciences and <sup>2</sup>Physiology, University of Kentucky, Lexington, Kentucky, USA. <sup>3</sup>Department of Ophthalmology, Yokohama City University, Yokohama, Japan. <sup>4</sup>Department of Plant & Soil Sciences, University of Kentucky, Lexington, Kentucky, USA. <sup>5</sup>Department of Anatomy and Cell Biology, Georg-August-University, Goettingen, Germany. <sup>6</sup>Department Gene Regulation and Differentiation, Helmholtz Centre for Infection Research, Braunschweig, Germany. <sup>7</sup>Department of Ophthalmology, University of Tokyo School of Medicine, Tokyo, Japan. <sup>8</sup>Department of Molecular and Cellular Physiology, Louisiana State University Health Sciences Center, Shreveport, Louisiana, USA. <sup>9</sup>Department of Microbiology, Immunology and Molecular Genetics, University of Kentucky, Lexington, Kentucky, USA. <sup>10</sup>Hamon Center for Therapeutic Oncology Research, University of Texas Southwestern Medical Center, Dallas, Texas, USA. <sup>11</sup>Division of Vascular Biology, Department of Physiology and Cell Biology, Kobe University Graduate School of Medicine, Kobe, Japan. <sup>12</sup>Department of Ophthalmology and Visual Sciences, Moran Eye Center, University of Utah School of Medicine, Salt Lake City, Utah, USA. <sup>13</sup>Department of Ophthalmology, Veterans Affairs Salt Lake City Healthcare System, Salt Lake City, Utah, USA. <sup>14</sup>These authors contributed equally to this work. Correspondence should be addressed to J.A. (jamba2@email.uky.edu).

Received 15 May; accepted 9 July; published online 9 August 2009; doi:10.1038/nm.2018

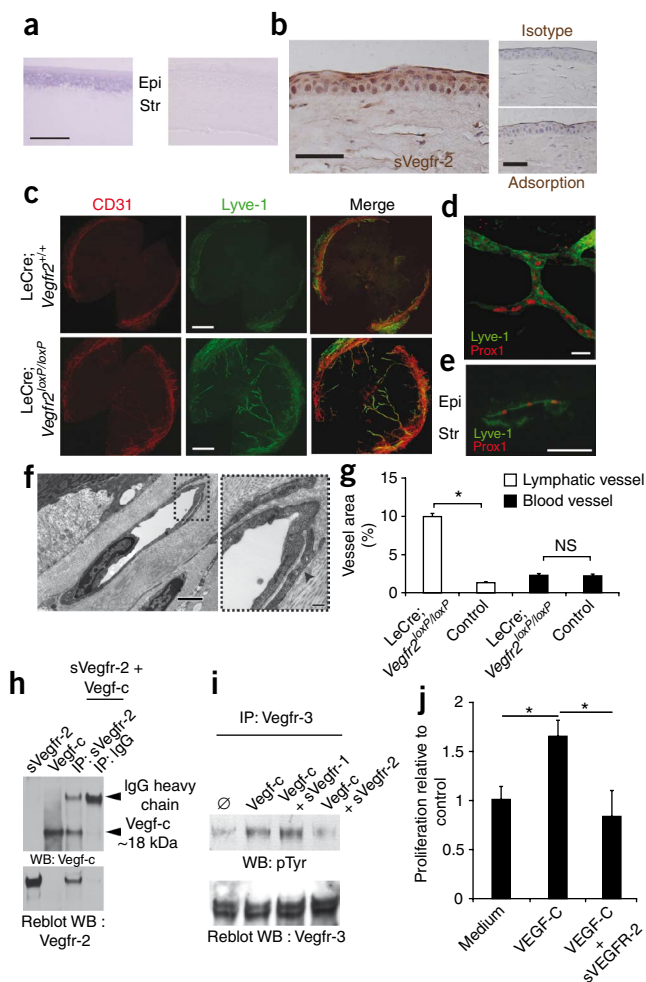


**Figure 1** Loss of endogenous sVegfr-2, which antagonizes Vegf-c, leads to spontaneous corneal lymphangiogenesis. **(a)** *sVegfr2* mRNA detection (purple-blue) by *in situ* hybridization in the mouse cornea. Epi, epithelium; Str, stroma. **(b)** sVegfr-2 immunolocalization (brown) in the mouse cornea by AA21127 antibody staining. Cell nuclei are stained blue by hematoxylin. Isotype, negative control rabbit IgG; adsorption, negative control with antibody preadsorbed with immunizing peptide. **(c)** Representative corneal flat mounts from a LeCre; *Vegfr2*<sup>loxP/loxP</sup> mouse ( $n = 30$ ). Lyve-1<sup>+</sup> (green) lymphatic and CD31<sup>+</sup> (red) Lyve-1<sup>-</sup> blood vessels are shown. **(d,e)** Immunofluorescent detection of Lyve-1<sup>+</sup> (green) Prox1<sup>+</sup> (red) lymphatic vessels in corneal whole mounts **(d)** and cross sections **(e)** from LeCre; *Vegfr2*<sup>loxP/loxP</sup> mice. **(f)** Transmission electron microscopy of a lymphatic vessel in the cornea of a LeCre; *Vegfr2*<sup>loxP/loxP</sup> mouse. Inset shows partly overlapping endothelial cells (arrowhead). **(g)** Quantification of vessel area in corneal flat mounts ( $n = 5$ –20 per group). **(h)** Representative western blot (WB) of samples of recombinant sVegfr-2 incubated with recombinant Vegf-c and immunoprecipitated (IP) with either antibody to Vegfr-2 (lane 3) antibody or isotype control IgG (lane 4) and immunoblotted with Vegf-c-specific antibody. Samples of sVegfr-2 and Vegf-c were loaded in lanes 1 and 2, respectively. In 'reblot WB', the same membrane was reprobed for Vegfr-2. **(i)** Representative immunoblot to detect Vegf-c-induced Vegfr-3 phosphorylation in mouse lymphatic endothelial cells treated with Vegf-c alone, Vegf-c and sVegfr-1 or Vegf-c and sVegfr-2. In 'reblot WB', the same membrane was reprobed for total Vegfr-3.  $\emptyset$ , medium only. pTyr, phosphorylated tyrosine antibody. **(j)** Proliferation of human lymphatic microvascular endothelial cells treated with or without VEGF-C and sVEGFR-2, as indicated, as quantified by BrdU uptake ( $n = 4$ ). NS, not significant; \* $P < 0.05$  by Mann-Whitney *U* test. Error bars depict means  $\pm$  s.e.m. Scale bars: 50  $\mu$ m **(a,b,d)**; 500  $\mu$ m **(c)**; 25  $\mu$ m **(e)**; 1  $\mu$ m **(f, left)**; 200 nm, **(f, right)**.

## RESULTS

### Cloning of sVegfr-2

During the course of our studies uncovering the nonredundant function of sVegfr-1 in corneal avascularity<sup>11</sup>, which is crucial for optimal vision, we observed, by western blotting, anomalous migration of a 75-kDa protein species that was immunoreactive to an antibody (T014; ref. 12) that recognizes the amino terminus of Vegfr-2 (Supplementary Fig. 1a). Given the similarity in the exon-intron structure between *Vegfr1* (official symbol *Flt1*) and *Vegfr2* (official symbol *Kdr*), we hypothesized that this unidentified protein represented a previously undescribed truncated form of the 230-kDa membrane-bound form of Vegfr-2 (mbVegfr-2) resulting from alternative splicing. Given that the lymphatic mitogen VEGF-C (ref. 13) is capable of binding mbVEGFR-2 (ref. 14), a truncated form of Vegfr-2 might have antilymphangiogenic activity.

We modeled the potential alternative splicing of *Vegfr2* on the basis of the alternative splicing that occurs in *Vegfr1* (ref. 8), and found that retention of intron 13 in the mature messenger RNA would yield a truncated transcript variant whose protein product would lack the transmembrane and intracellular tyrosine kinase domains of mbVegfr-2, owing to the presence of an in-frame termination TAA codon 39 nucleotides downstream from the exon 13–intron 13 junction (Supplementary Fig. 1c). To verify the existence of this soluble splicing variant in the mouse cornea, we devised primers targeting intron 13 and exon 12 (Supplementary Fig. 1c and Supplementary

Fig. 2a). Use of an exon 12-targeted primer allowed us to distinguish between amplification of mRNA-derived complementary DNA and genomic DNA contamination on the basis of amplicon size. PCR yielded a 393-base pair product spanning the location of the splicing event (Supplementary Fig. 1d). Bioinformatic analysis of intron 13 revealed three potential polyadenylation (polyA) signal sequences (Supplementary Fig. 1c). Using rapid amplification of cDNA 3' ends PCR, we found the third potential polyA signal at positions 3,956–3,961 to be functional (Supplementary Fig. 1c,e and Supplementary Fig. 2a). From mouse corneal mRNA, we cloned a cDNA containing a 2,022-base pair open reading frame encoding a polypeptide of 673 amino acids designated as sVegfr-2 (Supplementary Fig. 2b; the sequence of the sVegfr-2 transcript is shown in Supplementary Fig. 2a). This protein contains a 13-amino acid carboxyl-terminus sequence (Supplementary Fig. 1b) not present in mbVegfr-2 or in any other known protein and against which we raised a rabbit polyclonal antibody (AA21127; Supplementary Fig. 3).

### sVegfr-2 is expressed in and is essential for alymphatic cornea

This sVegfr-2 transcript was localized by *in situ* hybridization principally to the corneal epithelium (Fig. 1a). Immunolocalization using the AA21127 antibody in the newborn mouse showed the presence of sVegfr-2 in the corneal epithelium and stroma (Supplementary Fig. 4a). In the adult cornea, sVegfr-2 was more abundant in the epithelium than in the stroma (Fig. 1b and Supplementary Fig. 4a). sVegfr-2 was distributed uniformly in the cornea with enhanced expression near the limbus (Supplementary Fig. 4b). In contrast, sVegfr-2 did not immunolocalize in the conjunctiva (Supplementary Fig. 4b,c). We identified sVegfr-2 in the cornea as a 75-kDa species by western blotting using both the AA21127 and T014 antibodies (Supplementary Fig. 4d). However, we did not detect the 230-kDa mbVegfr-2 in the cornea by western blotting with T014 (Supplementary Fig. 1a) or by immunofluorescence with an antibody targeting the carboxyl terminus

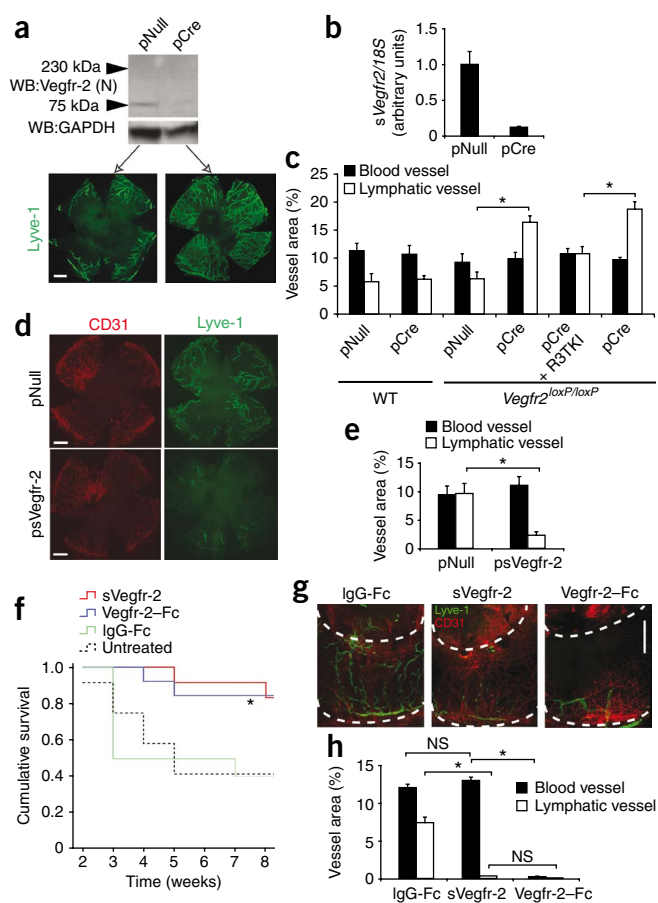


**Figure 2** sVegfr-2 inhibits reparative corneal lymphangiogenesis and rejection of corneal allografts. **(a)** Representative western blot, 5 d after suture placement in *Vegfr2<sup>loxP/loxP</sup>* mouse corneas treated with pCre or pNull ( $n = 8$  corneas pooled per group). Loading control, glyceraldehyde-3-phosphate dehydrogenase (GAPDH). N, amino terminus of Vegfr-2. The bottom images (arrows) show Lyve-1<sup>+</sup> vessels (green) 14 d after suture placement. **(b)** Real-time PCR quantitation of sVegfr-2 mRNA in *Vegfr2<sup>loxP/loxP</sup>* mouse corneas ( $n = 4$  per group). **(c)** Quantification of vessel area in corneal flat mounts from *Vegfr2<sup>loxP/loxP</sup>* and BALB/c wild-type (WT) mice ( $n = 5$  or 6 per group) and in corneal flat mounts from *Vegfr2<sup>loxP/loxP</sup>* mice injected intracorneally with pCre followed by systemic administration of a Vegfr-3 tyrosine kinase inhibitor (R3TKI) ( $n = 8$  per group). **(d)** Representative corneal flat mounts stained for CD31 (red) and Lyve-1 (green) of sutured eyes from C57BL/6J WT mice treated with psVegfr-2 or pNull. **(e)** Quantification of vessel area in flat mounts of sutured corneas from C57BL/6J WT mice treated with psVegfr-2 or pNull ( $n = 5$  per group). **(f)** Kaplan-Meier survival curves showing survival of corneal grafts in BALB/c hosts treated with sVegfr-2, Vegfr-2-Fc or IgG-Fc or left untreated ( $n = 10$ –13 per group). **(g)** Representative flat mounts of transplanted mouse corneas treated with sVegfr-2, Vegfr-2-Fc or IgG-Fc. Limbus, bottom dotted line; recipient-donor interface, top dotted line. **(h)** Quantification of corneal graft vessel area in flat mounts of transplants ( $n = 5$  per group). (NS, non-significant; \* $P < 0.05$  by Mann-Whitney  $U$  test. Error bars depict means  $\pm$  s.e.m. Scale bars, 500  $\mu$ m.

and lymphatic vessels is usually intertwined, we found it surprising that these corneas were not invaded by blood vessels, as indicated by the absence of CD31<sup>+</sup>Lyve-1<sup>-</sup> vessels (Fig. 1c,g). We confirmed this independently by demonstrating that the vessels in these corneas did not express MECA-32, a blood vessel-specific marker (Supplementary Fig. 6c,d). All littermate control corneas ( $n = 30$ ) were, like those of wild-type mice, devoid of both lymphatic and blood vessels (Fig. 1c and Supplementary Fig. 6d). LeCre;*Vegfr2<sup>loxP/loxP</sup>* mice had normal limbal blood vessel morphology and an unimpaired corneal hemangiogenesis response to suture injury (Supplementary Fig. 6d,e), confirming intact vascular endothelial cell Vegfr-2 function.

### sVegfr-2 is a Vegf-c antagonist

These results indicate that the developing mouse cornea is exposed to prolymphangiogenic stimuli that are counterbalanced by sVegfr-2 to create an alymphatic cornea. Indeed, wild-type P0 corneas, unlike adult corneas, showed Vegf-c expression (Supplementary Fig. 7). We reasoned that sVegfr-2 ablation led to spontaneous corneal lymphangiogenesis because of the ability of sVegfr-2 to bind Vegf-c and thereby inhibit its function. Indeed, the amounts of sVegfr-2 (1,655.8  $\pm$  44.62 pg per mg of total protein) in wild-type P0 cornea were sufficiently in excess of Vegf-c (45.4  $\pm$  3.2 pg per mg of total protein) to fulfill a trapping function. sVegfr-2, which contains the Vegf-c-binding immunoglobulin-like domain-2 of mbVegfr-2 (ref. 18), interacted with Vegf-c, as determined by immunoprecipitation, and inhibited both Vegfr-3 phosphorylation and proliferation of lymphatic endothelial cells (LECs) stimulated by VEGF-C (Fig. 1h–j). Also, Vegf-c-induced corneal lymphangiogenesis was inhibited by intracorneal administration<sup>11</sup> of a plasmid encoding sVegfr-2 (psVegfr-2) (Supplementary Fig. 8). Collectively, these data are consistent with a model in which sVegfr-2 acts as an endogenous sink for Vegf-c during corneal development and thereby establishes an alymphatic cornea.

Consistent with the report that mouse Vegfr-2 binds human VEGF-D but not mouse Vegf-d (ref. 19), psVegfr-2 inhibited corneal lymphangiogenesis induced by human VEGF-D but not mouse Vegf-d (Supplementary Fig. 8). Also, unlike Vegf-c, Vegf-d was not expressed in the newborn mouse cornea (Supplementary Fig. 9), consistent with the idea that sVegfr-2 maintains the alymphatic nature of the cornea.

of mbVegfr-2, which is not present in sVegfr-2 (Supplementary Fig. 4e). Neither did we detect the mbVegfr-2 transcript in the cornea by RT-PCR (Supplementary Fig. 4f). Thus, the mouse cornea expresses sVegfr-2 but not mbVegfr-2.

To define the function of sVegfr-2 in the cornea, we targeted it using multiple strategies. Because *Vegfr2<sup>-/-</sup>* mice die *in utero*<sup>15</sup>, we ablated corneal sVegfr-2 expression using a Cre-*loxP* strategy. This strategy enabled the specific targeting of sVegfr-2, because mbVegfr-2 is not expressed in the cornea (Supplementary Fig. 4e,f). We created *Vegfr2<sup>loxP/loxP</sup>* mice by targeting exon 1 (Supplementary Fig. 5) and interbred them with LeCre mice that constitutively and uniformly express Cre recombinase in the cornea under the control of a paired box-6 promoter<sup>16</sup>. Mice of all genotypes were born at the expected mendelian ratios and were macroscopically indistinguishable from one another. However, all LeCre;*Vegfr2<sup>loxP/loxP</sup>* mouse corneas ( $n = 30$ ), which lacked sVegfr-2 expression (Supplementary Fig. 6a), were densely covered with lymphatic vessels at postnatal day 0 (P0) (Fig. 1c). We identified these vessels as lymphatics by virtue of their intense lymphatic vessel endothelial receptor-1 (Lyve-1) reactivity, moderate CD31 reactivity, nuclear prospero homeobox-1 (Prox1) expression and blind-ended morphology (Fig. 1c–e and Supplementary Fig. 6b). Although Lyve-1<sup>+</sup> macrophages have been described in the cornea<sup>17</sup>, coexpression of Prox1 in these vessels confirmed their identity as lymphatics (Fig. 1d,e). Furthermore, ultrastructural examination showed that these vessels lacked erythrocytes, did not have a continuous basement membrane and contained partly overlapping thin endothelial cells free of pericyte coverage—all features typical of lymphatics (Fig. 1f). Because the growth of blood

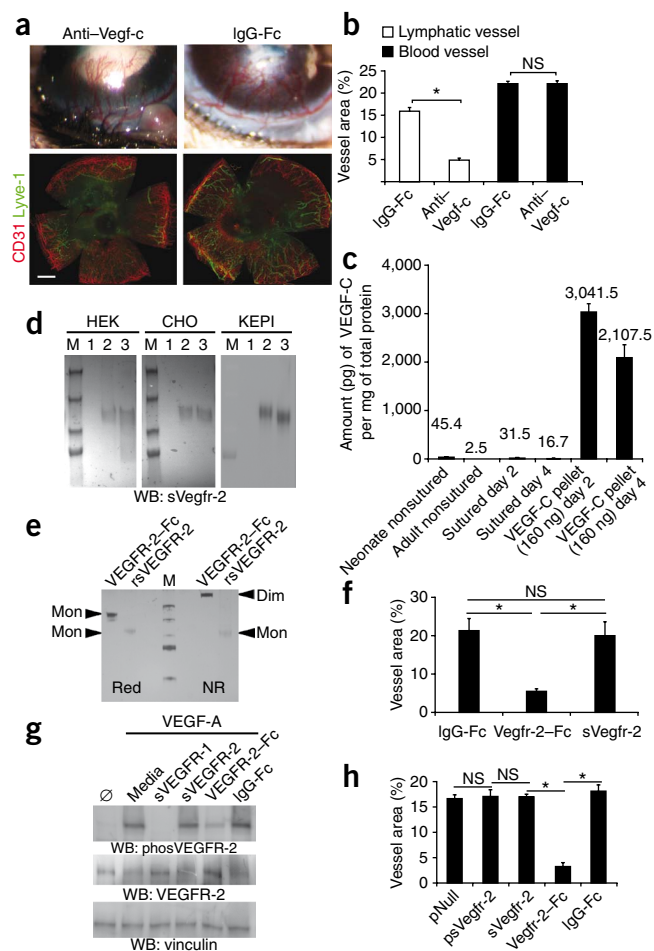


**Figure 3** Endogenous Vegf-c and sVegfr-2 selectively modulate corneal lymphangiogenesis. **(a)** Representative color photographs of sutured WT mouse corneas (top) and representative flat mounts of sutured corneas stained for CD31 (red) and Lyve-1 (green) (bottom). Scale bar, 500  $\mu$ m. **(b)** Quantification of corneal vessel area of sutured corneas of WT mice treated with a Vegf-c-neutralizing antibody or IgG-Fc isotype control. Anti-Vegf-c, Vegf-c-specific antibody. **(c)** ELISA quantification in C57BL/6J mouse corneas of mouse Vegf-c 2 and 4 d after suture placement or of human VEGF-C after implantation of pellets containing 160 ng recombinant human VEGF-C. ELISAs are not expected to cross react ( $n = 3$ ). **(d)** Immunoblotting of sVegfr-2 secreted by transfected human embryonic kidney cells (HEK), Chinese hamster ovary cells (CHO) and mouse corneal epithelial cells (KEPI) under reducing and nonreducing conditions. M, marker; lane 1, pNull; lane 2, psVegfr-2 (reducing); lane 3, psVegfr-2 (nonreducing). **(e)** Silver staining of a polyacrylamide gel loaded with VEGFR-2-Fc and recombinant sVEGFR-2 (rsVEGFR-2) and resolved under reducing (Red) versus nonreducing (NR) conditions. Dim, dimer; Mon, monomer. **(f)** Corneal area occupied by blood vessels (CD31+Lyve-1<sup>-</sup>) after suture injury in WT mice treated with IgG-Fc, Vegfr-2-Fc or sVegfr-2 ( $n = 3$ –5 per group). **(g)** Representative immunoblot of phosphorylated VEGFR-2 (phosVEGFR-2) in porcine aortic endothelial cells stably transfected with human VEGFR-2 and stimulated with VEGF-A. Reblotting for total VEGFR-2 and vinculin are shown.  $\emptyset$ , no VEGF-A. **(h)** Corneal area occupied by blood vessels (CD31+Lyve-1<sup>-</sup>) after pVegf-a injection and injection with the indicated plasmids or proteins. ( $n = 4$  per group) **(b,c,f,h)**. \* $P < 0.05$  by Mann-Whitney  $U$  test. Error bars depict means  $\pm$  s.e.m.

corneal transplantation. A single intracorneal administration of a dimeric Vegfr-2-Fc fusion protein more than doubled the transplant survival rate (a 105% and 101% increase compared to IgG-Fc and no treatment, respectively;  $P < 0.05$ ,  $n = 10$ –13 mice per group; **Fig. 2f**). The markedly lower rejection rate induced by Vegfr-2-Fc administration (75% compared to IgG-Fc treatment and 74% compared to no treatment) is consistent with the observed reduction in blood vessel and lymphatic sprouting through the donor-recipient interface (**Fig. 2g,h**). To our surprise, a single intracorneal administration of monomeric sVegfr-2 induced the same degree of corneal allograft survival as did dimeric Vegfr-2-Fc, despite reducing sprouting of only lymphatic vessels through the donor-recipient interface (blood vessels were not affected; **Fig. 2f–h**). These data suggest that inhibition of lymphatic vessels impairs the establishment of the draining route through which immune cells are trafficked<sup>23–25</sup> and is sufficient to enhance corneal allograft survival.

### Endogenous Vegf-c promotes lymphangiogenesis

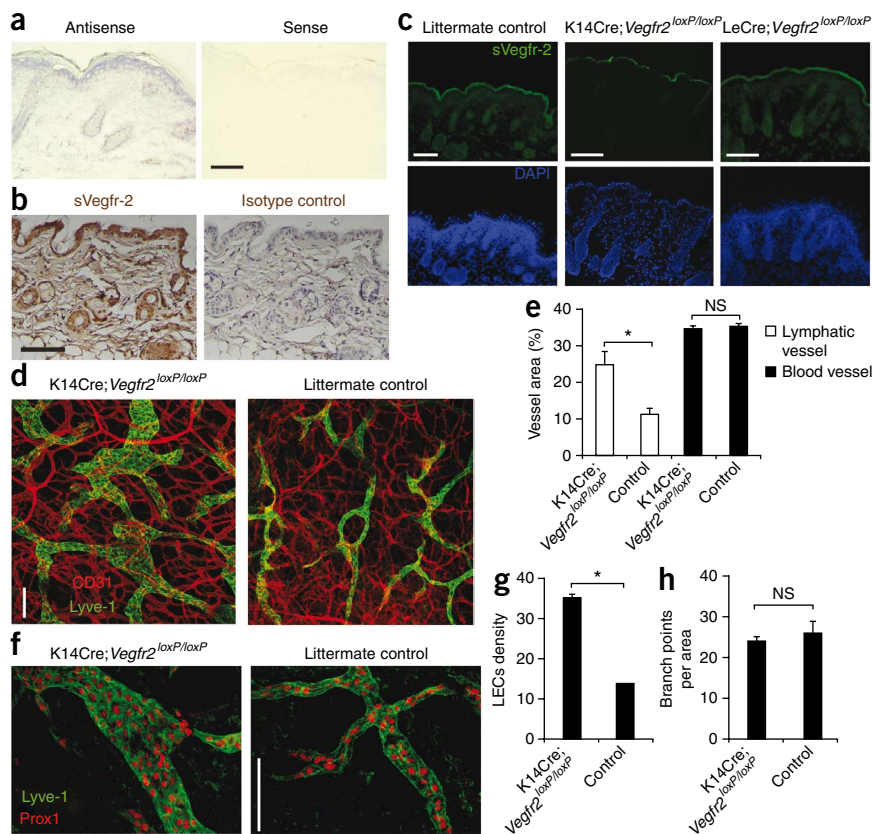
Selective lymphangiogenesis inhibition by sVegfr-2 is consistent with the selective effect of endogenous Vegf-c on the lymphatic vasculature<sup>6,13,26–28</sup>. However, implantation of pellets containing 160–200 ng of recombinant human VEGF-C into the mouse cornea has been reported to induce hemangiogenesis<sup>29–32</sup>. To reconcile these findings, we injected neutralizing Vegf-c-specific antibodies into the corneas of wild-type mice after suture injury and found that this resulted in inhibition of lymphangiogenesis ( $P < 0.05$ ,  $n = 8$ ) but not hemangiogenesis (**Fig. 3a,b**). These data show that endogenous Vegf-c selectively promotes lymphangiogenesis in the cornea and help explain the selective effect of sVegfr-2. The lack of Vegfr-3 expression in conjunctival and corneal blood vessels<sup>33,34</sup> also supports a model in which endogenous Vegf-c binds Vegfr-3 on lymphatic vessels preferentially compared to Vegfr-2 on blood vessels in these tissues on the basis of relative receptor affinities<sup>35</sup>. Also, Vegf-c is far less efficient at activating Vegfr-2 than is Vegf-a<sup>36</sup>, the principal driver of corneal hemangiogenesis<sup>11,32</sup>.

### sVegfr-2 inhibits lymphangiogenesis and transplant rejection

To determine the function of sVegfr-2 in the adult, we studied a clinically relevant mouse model of suture-induced corneal neovascularization<sup>20</sup>. Suture injury increased corneal sVegfr-2 expression (in the epithelium but not in infiltrating macrophages) in wild-type mice (**Supplementary Fig. 10**). Ablation of sVegfr-2 expression by intracorneal administration<sup>11</sup> of a plasmid coding for Cre recombinase (pCre) in *Vegfr2<sup>loxP/loxP</sup>* mice markedly increased suture-induced lymphangiogenesis but not hemangiogenesis compared to empty vector (pNull) administration by 161%  $\pm$  9% ( $P < 0.05$ ,  $n = 5$  mice per group) (**Fig. 2a–c**). This outstripping of hemangiogenesis by lymphangiogenesis suggests that induction of endogenous sVegfr-2 expression by injury is a compensatory antilymphangiogenic response. Both pCre-injected and pNull-injected corneas of wild-type mice showed similar degrees of lymphangiogenesis after suture injury, excluding a nonspecific effect of Cre recombinase (**Fig. 2c**). pCre-induced enhancement of suture-induced lymphangiogenesis in *Vegfr2<sup>loxP/loxP</sup>* mice was reduced by a Vegfr-3 tyrosine kinase inhibitor<sup>21</sup>, supporting the concept that endogenous sVegfr-2 is an *in vivo* Vegf-c antagonist (**Fig. 2c**). Conversely, augmentation of sVegfr-2 expression using *in vivo* transfection<sup>11</sup> of wild-type mouse corneas with psVegfr-2, but not pNull, reduced suture injury-induced lymphangiogenesis but not hemangiogenesis by 76%  $\pm$  6% ( $P < 0.05$ ,  $n = 5$  mice per group) (**Fig. 2d,e**).

Because lymphangiogenesis has been implicated in corneal allograft rejection<sup>22</sup>, we studied the function of sVegfr-2 in a mouse model of

**Figure 4** Loss of *sVegfr2* in the skin induces lymphatic hyperplasia. **(a)** *sVegfr2* mRNA detection (purple-blue) by *in situ* hybridization in the mouse skin. Antisense, antisense probe; Sense, sense probe (negative control). **(b)** *sVegfr-2* immunolocalization (brown) in mouse skin using the AA21127 antibody. Cell nuclei are stained blue by hematoxylin. **(c)** Immunofluorescence of *sVegfr-2* (green) in the skin of newborn mice. Superficial keratin autofluorescence is seen in all instances. Cell nuclei are stained with DAPI. **(d)** Representative whole mounts of the ventral skin of P0 mice. Lyve-1<sup>+</sup> (green) lymphatic and CD31<sup>+</sup> (red) Lyve-1<sup>-</sup> blood vessels are shown. **(e)** Skin area occupied by blood vessels (CD31<sup>+</sup>Lyve-1<sup>-</sup>) and lymphatic vessels (Lyve-1<sup>+</sup>) in P0 mice of the indicated genotypes or their littermate controls ( $n = 14$ ). **(f)** Representative whole-mount immunofluorescent image showing Lyve-1<sup>+</sup> (green) and Prox1<sup>+</sup> (red) lymphatic vessels of P0 mice ( $n = 14$  per group). **(g)** LEC density, quantified by the number of Prox1<sup>+</sup> nuclei per 100  $\mu\text{m}$  of lymphatic vessel (Lyve-1<sup>+</sup>) length, in P0 mice ( $n = 12$ –14 per group). **(h)** Quantitative branch-point analysis of Lyve-1<sup>+</sup> lymphatic vessels per unit area ( $750 \mu\text{m} \times 750 \mu\text{m}$ ) ( $n = 8$  per group). Scale bars, 50  $\mu\text{m}$ . \* $P < 0.05$  by Mann-Whitney  $U$  test. Error bars depict means  $\pm$  s.e.m.



We quantified VEGF-C abundance after implanting a 160-ng VEGF-C pellet and found that this resulted in corneal VEGF-C levels that were 100–125 times greater than those observed after suture injury and 45–66 times greater than levels in neonatal corneas (Fig. 3c). Such exaggerated amounts of VEGF-C, which are supraphysiological and far greater than those achieved in pathophysiologically relevant states, could explain the reported hemangiogenic effects of exogenous VEGF-C.

### Monomeric *sVegfr-2* does not block hemangiogenesis

The selective effect of *sVegfr-2* in inhibiting lymphangiogenesis but not hemangiogenesis was unexpected, because mbVegfr-2 is capable of binding Vegf-a, which promotes hemangiogenesis. To explain this selectivity, we first sought to determine whether *sVegfr-2* exists in monomeric or dimeric form, because a recombinant form of the ecto-domain of mbVEGFR-2 has been shown to be a monomer that has little or no affinity for VEGF-A compared to a dimeric recombinant VEGFR-2-Fc fusion protein<sup>37–39</sup>. We found that *sVegfr-2* secreted by mouse corneal epithelial cells, human embryonic kidney cells and Chinese hamster ovary cells, as well as recombinant *sVEGFR-2*, all migrated at equivalent apparent molecular masses under both non-reducing and reducing conditions of western blotting, data consistent with its existence as a monomer (Fig. 3d,e). In contrast, the migration of VEGFR-2-Fc was consistent with it being a dimer (Fig. 3e).

Next, we tested the effects of monomeric *sVegfr-2* and dimeric *Vegfr-2*-Fc on models of corneal neovascularization induced by injury or Vegf-a treatment. Suture-induced corneal hemangiogenesis, which is driven principally by upregulation of endogenous Vegf-a<sup>32</sup>, was inhibited by *Vegfr-2*-Fc but not *sVegfr-2* (Fig. 3f). Similarly, VEGF-A-induced phosphorylation of mbVEGFR-2 in porcine aortic endothelial cells was inhibited by VEGFR-2-Fc but not *sVEGFR-2*, and Vegf-a-induced corneal hemangiogenesis was inhibited by *Vegfr-2*-Fc but not by *sVegfr-2* or psVegfr-2 (Fig. 3g,h). These functional

data provide a mechanistic basis for the absence of an antihemangiogenic effect of endogenous *sVegfr-2* and corroborate the previously reported *in vitro* differential VEGF-A binding avidity between monomeric and dimeric forms of VEGFR-2.

### Nonocular role of *sVegfr-2*

We detected *sVegfr2* mRNA expression by northern blotting of poly A-enriched RNA isolated from various mouse organs (Supplementary Fig. 11), suggesting that *sVegfr-2* might have functions outside of the eye. *sVegfr2* mRNA was abundant in the alymphatic epidermis of the skin as well as in the hair follicles of wild-type mice (Fig. 4a). *sVegfr-2* protein was immunolocalized in the epidermis, hair follicles and, consistent with its ability to diffuse, also in the dermis of wild-type mice (Fig. 4b). In contrast, mbVegfr-2 was expressed in the skin vasculature but not in epithelial cells or hair follicles (Supplementary Fig. 12a). As in the cornea, Vegf-c was expressed in P0 wild-type mouse skin but was undetectable in adult skin (Supplementary Fig. 12b). Excess VEGF-C in the skin, achieved by either transgenic overexpression or implantation of VEGF-C-overexpressing cells, leads to hyperplasia but not sprouting of lymphatic vessels<sup>13,40</sup>. To determine the function of *sVegfr-2* in the skin, we interbred *Vegfr2*<sup>loxP/loxP</sup> mice with K14Cre mice that constitutively and uniformly express Cre recombinase in the epidermis and hair follicles<sup>41</sup>. This strategy specifically targets *sVegfr-2*, because the epidermis and hair follicles express *sVegfr-2* but not mbVegfr-2. Notably, in the skin of all P0 K14Cre;*Vegfr2*<sup>loxP/loxP</sup> mice, which lacked *sVegfr-2* expression (Fig. 4c), there was marked enlargement of lymphatic vessels compared to those in the skin of littermate controls (Fig. 4d–f). The dilated lymphatics in the skin of K14Cre-*Vegfr2*<sup>loxP/loxP</sup> mice were also hyperplastic (Fig. 4e,g). However, the density of lymphatic structures, as quantified by branch

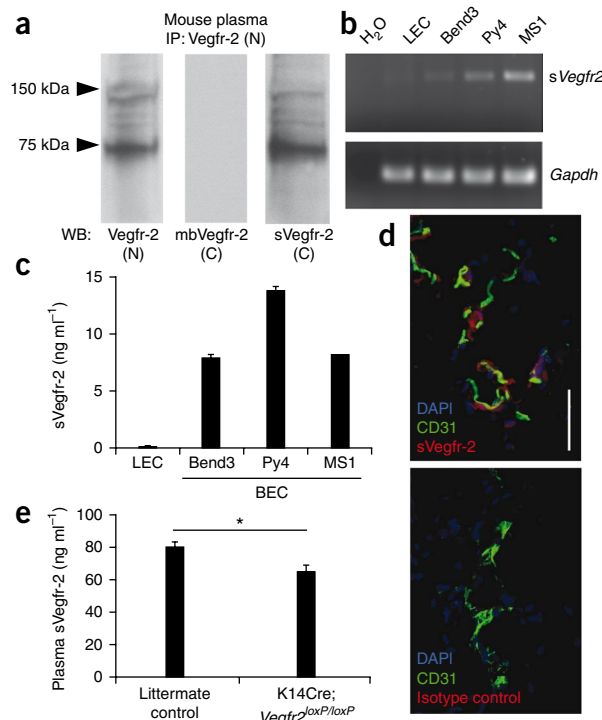


**Figure 5** sVegfr-2 is produced by BECs and skin epithelium and circulates in plasma. (a) Representative western blots of mouse plasma immunoprecipitated with an antibody against the amino terminus of Vegfr-2 (Vegfr-2 (N)) and immunoblotted with either the same antibody (left), antibody to the carboxyl terminus of sVegfr-2 (sVegfr-2 (C); right) or an antibody against the carboxyl terminus of mbVegfr-2 (mbVegfr-2 (C); center). (b) PCR amplification of sVegfr2 mRNA using cDNA derived from mouse LECs and mouse BECs isolated from the brain (Bend3), Skin (Py4) or pancreas (MS1). The first lane (H<sub>2</sub>O) shows a template-negative control. Gapdh was the loading control ( $n = 5$ ). (c) ELISA quantification of sVegfr-2 protein in the supernatant of blood and lymphatic endothelial cells ( $n = 3$  per group). (d) Immunofluorescence of sVegfr-2 or isotype control antibody (red) and CD31 (green) in the pulmonary microvasculature. Cell nuclei are stained with DAPI. Scale bar, 50  $\mu$ m. (e) ELISA quantification of sVegfr-2 concentration in plasma ( $n = 7-9$  per group). \* $P < 0.05$  by Mann-Whitney  $U$  test. Error bars depict means  $\pm$  s.e.m.

of mbVegfr-2 (Fig. 5a), suggesting that circulating Vegfr-2 is encoded by the sVegfr2 splice variant. Mouse blood endothelial cell (BEC) lines derived from the microvasculature of the brain, pancreas, or skin all synthesized and secreted sVegfr-2, far in excess of its production by LECs (Fig. 5b,c). sVegfr-2 was also detected by immunofluorescence using AA21127 in mouse lung microvasculature, identifying BECs as sources of plasma sVegfr-2 (Fig. 5d). The production of antilymphangiogenic sVegfr-2 by BECs could be one of the mechanisms underlying the observation that lymphangiogenesis typically lags behind hemangiogenesis in many neovascular models. To our surprise, plasma concentrations of sVegfr-2 were significantly lower in K14Cre;Vegfr2<sup>loxP/loxP</sup> mice compared to littermate controls (Fig. 5e), suggesting that skin epithelium is also a source of circulating sVegfr-2. An earlier report showing that K14Cre-driven expression of recombinant soluble VEGFR-3 leads to measurable circulating levels of the engineered protein<sup>27</sup> supports the concept that endogenous skin-derived sVegfr-2 can enter the circulation.

#### Human sVEGFR-2 inhibits lymphangioma cellular proliferation

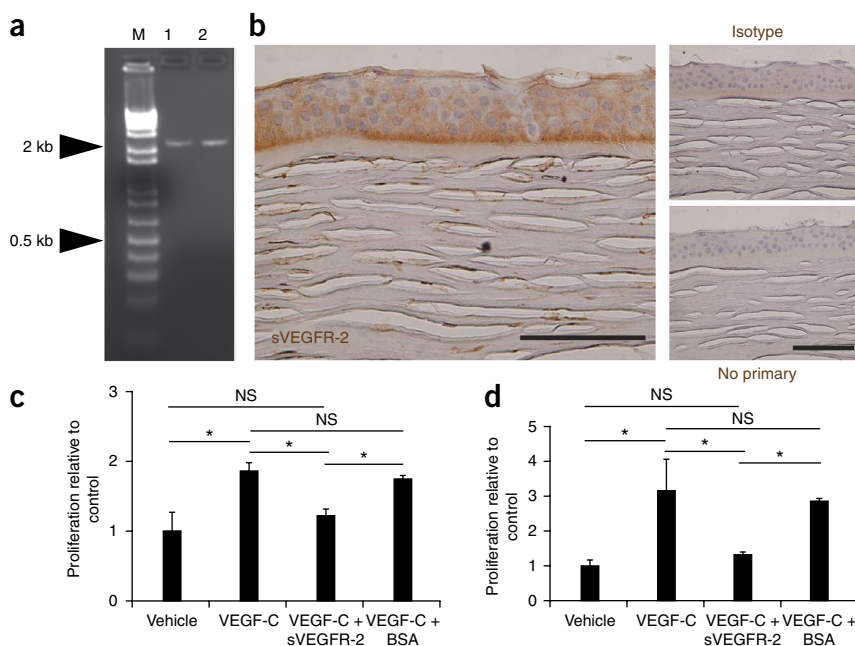
We confirmed the existence of an mRNA by encoding sVEGFR-2 from human umbilical vein endothelial cells by using RT-PCR to clone

point analysis, was not higher in K14Cre;Vegfr2<sup>loxP/loxP</sup> mice (Fig. 4h), just as in mouse skin exposed to excess VEGF-C<sup>13,40</sup>. In contrast to the changes in lymphatic architecture, there was no increase in skin blood vessel diameter or density in K14Cre;Vegfr2<sup>loxP/loxP</sup> mice (Fig. 4d,e). Lack of sVegfr-2 in the skin thus recapitulates the effects of VEGF-C overexpression—lymphatic hyperplasia—supporting the concept that sVegfr-2 is an *in vivo* antagonist of Vegf-c.

A protein immunoreactive to an antibody recognizing the amino terminus of Vegfr-2 has been detected in plasma and shown to be a surrogate biomarker of tumor growth<sup>42-44</sup>. However, its molecular identity (whether it is encoded by a splice variant of Vegfr2 or derived from ectodomain shedding or proteolytic cleavage of mbVegfr-2) and cellular source have been elusive. Circulating Vegfr-2 in plasma was immunoreactive to both the AA21127 and T014 antibodies but not to an antibody recognizing the carboxyl terminus

#### Figure 6 sVEGFR-2 exists in humans and inhibits human lymphangioma cell proliferation.

(a) PCR cloning of the open reading frame of VEGFR2 from human umbilical vein endothelial cells. M, marker; lanes 1 and 2 represent two independent amplification reactions. (b) sVEGFR-2 immunolocalization (brown) in human cornea using the AA21129 antibody. Cell nuclei are stained blue by hematoxylin. Isotype, negative control rabbit IgG; no primary, negative control with omission of primary antibody. (c,d) Proliferation of lymphatic endothelial cells isolated from two children with lymphangioma, stimulated by VEGF-C and treated with sVEGFR-2 or BSA, quantified by BrdU uptake ( $n = 6-9$  per group). (c) Cells from a 4-month-old child; (d) cells from a 10-month-old child. \* $P < 0.05$  by Mann-Whitney  $U$  test. Error bars depict means  $\pm$  s.e.m.



a cDNA containing a 2,159–base pair open reading frame (Fig. 6a). As with mouse *sVegfr2*, this mRNA resulted from retention of intron 13 containing an in-frame termination stop codon. Translation of the truncated *VEGFR2* mRNA results in a protein containing 679 amino acids with a unique 16–amino acid carboxyl-terminus sequence not present in mbVEGFR-2 and against which we generated a polyclonal antibody (AA21129, **Supplementary Fig. 13**). sVEGFR-2 was expressed in human cornea with a distribution similar to that in mice (Fig. 6b), suggesting that it has a similar role in maintaining an alymphatic state.

We tested the potential antilymphangiogenic property of human sVEGFR-2 *in vitro*. Lymphangioma is a common disfiguring childhood neoplasia whose etiology is unknown. Human lymphangioma endothelial cells (LaECs) produce VEGF-C and express VEGFR-3 (refs. 45–47), suggesting that their growth might be inhibited by disrupting this axis. Previously, we described the isolation of LaECs from axillary lymphangiomas in two human infants<sup>47</sup>. We found that sVEGFR-2 abolished VEGF-C–induced proliferation of both of these LaEC samples (Fig. 6c,d), raising the noteworthy possibility that these pediatric tumors could be molecularly targeted.

## DISCUSSION

As an endogenous uncoupler of the intertwined blood and lymphatic circulatory systems, sVegfr-2 represents a new molecular tool to selectively dissect the individual contributions of these parallel vasculatures in development and disease. Additionally, the identification of sVegfr-2 might enable new therapeutic strategies by selectively modulating aberrant lymphatic proliferation without causing the potential adverse effects of nonspecific antiangiogenic therapy.

The potential therapeutic value of selective lymphangiogenesis suppression is nowhere more apparent than in the setting of lymphangioma, which occurs in roughly 1 in 50 children<sup>48</sup>. These tumors, although classified as benign, can be locally invasive and quite disfiguring. Their pediatric preponderance highlights the need to develop selective antilymphangiogenic therapy. Our finding that sVEGFR-2 can prevent VEGF-C–induced proliferation of human lymphangioma endothelial cells raises the possibility that these pediatric tumors could be targeted on a molecular level.

Our discovery of sVEGFR-2 in the cornea endorses this tissue as a rich source of angiogenesis modulators and extends the concept of opposing molecular mechanisms regulating blood vessel growth<sup>7</sup> to lymphatics. Just as sVegfr-1 is required for corneal avascularity<sup>11,49</sup>, we now show that sVegfr-2 is essential for corneal alymphaticity. The presence of both sVegfr-1 and sVegfr-2 in the cornea attests to the necessity of impeding both blood and lymphatic vessel growth to preserve optical clarity and relative immunological privilege. Notably, these tandem traps are generated by a common mechanism involving alternative splicing.

The unexpected finding that sVegfr-2 enhances corneal allograft survival despite not inhibiting hemangiogenesis suggests that impairment of the establishment of lymphatic vascular drainage<sup>23,24</sup> alone is sufficient to enhance corneal allograft survival. Notably, the rate of allograft survival after a single local administration of sVegfr-2 was at least as high as the rate of survival induced by multiple systemic administrations of a VEGFR-3 antagonist in a previous study<sup>25</sup>. Apart from reducing lymphangiogenesis, it is also possible that sVegfr-2 promotes allograft survival by inhibiting Vegf-c–induced Vegfr-3 signaling in corneal dendritic cells and preventing their transmigration into the draining lymph node<sup>25</sup>. In addition to suggesting that sVegfr-2 administration could be a new therapeutic strategy for

improving survival of corneal transplants, the most common type of solid organ transplantation, our data provide a mechanistic basis for studying the effect of specific lymphangiogenesis suppression in other transplants, such as kidney, whose rejection is associated with lymphangiogenesis<sup>50</sup>.

Unlike other reported endogenous inhibitors of lymphangiogenesis (collagen XVIII fragments, semaphorin 3F and transforming growth factor- $\beta^{51-54}$ ), native sVegfr-2 is a specific and direct lymphangiogenesis inhibitor. An explanation for this specificity is that native sVegfr-2 exists as a monomer that, unlike dimeric mbVegfr-2, has poor avidity for Vegf-a. Nevertheless, we cannot exclude a minor antihemangiogenic role for sVegfr-2. Such a role might be masked by dominant effects of coexisting molecules, such as sVegfr-1, that have a much greater affinity for Vegf-a; in addition, such a role might become evident in experimental contexts where high levels of exogenous Vegf-c promote hemangiogenesis. A complete molecular understanding of the specific inhibition by endogenous sVegfr-2 of Vegf-c but not Vegf-a must await detailed structural studies of the Vegfr-2 ectodomain alone and in complexes with Vegf-a and Vegf-c. Collectively, our findings demonstrate that sVegfr-2 is a broad and nonredundant physiological regulator of lymphatic vessels. Further studies will reveal whether sVegfr-2 can arrest solid tumor lymphangiogenesis and metastasis, which can be promoted by VEGF-C overexpression<sup>55-57</sup> and inhibited by blocking Vegf-c activity<sup>58,59</sup>.

## METHODS

Methods and any associated references are available in the online version of the paper at <http://www.nature.com/naturemedicine/>.

**Accession codes.** The sVegfr2 and sVEGFR2 sequences are deposited in GenBank with accession numbers EU884114 and FJ899739.

*Note: Supplementary information is available on the Nature Medicine website.*

## ACKNOWLEDGMENTS

We thank R. Ashery-Padan (Tel Aviv University), P. Gruss (Max Planck Institute) and D.C. Beebe (Washington University) for LeCre mice, R.K. Nordeen (University of Colorado) for Cre plasmid, K. Miyazono (University of Tokyo) for pVegf-c and J.L. Arbisser (Emory University) and C.D. Kontos (Duke University) for endothelial cell lines; R. King, L. Xu, M. McConnell, K. Emerson, A. Blanford, M. Baker, S. Furlow, M. LaFalce and C. Long for technical assistance; and R. Mohan, F. Cambi, S. Bondada, M. Detmar, M.W. Fannon, T.V. Getchell, R.K. Jain, T.S. Khurana, B.J. Raisler, J.E. Springer, P.A. Pearson, C.W. Vander Kooi, J.G. Woodward, A.M. Rao, G.S. Rao, K. Ambati and L. Garcia for valuable discussions. This work was supported by US National Institutes of Health and National Eye Institute grants EY015422, EY018350 and EY018836 to J.A. and EY017182 and EY017950 to B.K.A.; a Research to Prevent Blindness Lew R. Wassermann Merit Award (J.A.); Physician Scientist Awards (J.A., B.K.A.); a Medical Student Fellowship (R.J.C.A.); a departmental unrestricted grant (J.A.); a University of Kentucky University Research Professorship (J.A.); Fight for Sight (R.J.C.A.); Japan Society for the Promotion of Science for Young Scientists (A.T.); a VA Merit Award (B.K.A.); and the US Department of Defense (B.K.A.). J.A. is also supported by the Doris Duke Distinguished Clinical Scientist Award and the Burroughs Wellcome Fund Clinical Scientist Award in Translational Research and is the Dr. E. Vernon Smith and Eloise C. Smith Macular Degeneration Endowed Chair.

## AUTHOR CONTRIBUTIONS

R.J.C.A., T.H., W.G.C., M.E.K., S.D., A.T., J.Z.B., K.Y., H.K., M.G.G. and S.C. designed and conducted experiments. R.A.B., J.W., H.A.W. and J.S.A. provided reagents and, with J.C., S.Y., S.A., N.M., M.L.P., M.H., T.U. and B.K.A., participated in planning experiments. J.A. conceived of and directed the project. R.J.C.A. and J.A. wrote the manuscript. All authors had the opportunity to discuss the results and comment on the manuscript.

## COMPETING INTERESTS STATEMENT

The authors declare competing financial interests: details accompany the full-text HTML version of the paper at <http://www.nature.com/naturemedicine/>.

1. Ferrara, N. & Kerbel, R.S. Angiogenesis as a therapeutic target. *Nature* **438**, 967–974 (2005).
2. Carmeliet, P. Angiogenesis in life, disease and medicine. *Nature* **438**, 932–936 (2005).
3. Fenwick, A. Waterborne infectious diseases—could they be consigned to history? *Science* **313**, 1077–1081 (2006).
4. Carmeliet, P. *et al.* Abnormal blood vessel development and lethality in embryos lacking a single *Vegf* allele. *Nature* **380**, 435–439 (1996).
5. Ferrara, N. *et al.* Heterozygous embryonic lethality induced by targeted inactivation of the *Vegf* gene. *Nature* **380**, 439–442 (1996).
6. Karkkainen, M.J. *et al.* Vascular endothelial growth factor C is required for sprouting of the first lymphatic vessels from embryonic veins. *Nat. Immunol.* **5**, 74–80 (2004).
7. Folkman, J. Angiogenesis in cancer, vascular, rheumatoid and other disease. *Nat. Med.* **1**, 27–31 (1995).
8. Kendall, R.L. & Thomas, K.A. Inhibition of vascular endothelial cell growth factor activity by an endogenously encoded soluble receptor. *Proc. Natl. Acad. Sci. USA* **90**, 10705–10709 (1993).
9. Sela, S. *et al.* A novel human-specific soluble vascular endothelial growth factor receptor 1: cell-type-specific splicing and implications to vascular endothelial growth factor homeostasis and preeclampsia. *Circ. Res.* **102**, 1566–1574 (2008).
10. Rajakumar, A. *et al.* Novel soluble Flt-1 isoforms in plasma and cultured placental explants from normotensive pregnant and preeclamptic women. *Placenta* **30**, 25–34 (2009).
11. Ambati, B.K. *et al.* Corneal avascularity is due to soluble *Vegf* receptor-1. *Nature* **443**, 993–997 (2006).
12. Huang, X., Gottstein, C., Brekken, R.A. & Thorpe, P.E. Expression of soluble *Vegf* receptor 2 and characterization of its binding by surface plasmon resonance. *Biochem. Biophys. Res. Commun.* **252**, 643–648 (1998).
13. Jeltsch, M. *et al.* Hyperplasia of lymphatic vessels in VEGF-C transgenic mice. *Science* **276**, 1423–1425 (1997).
14. Joukov, V. *et al.* A novel vascular endothelial growth factor, VEGF-C, is a ligand for the Flt4 (VEGFR-3) and KDR (VEGFR-2) receptor tyrosine kinases. *EMBO J.* **15**, 290–298 (1996).
15. Shalaby, F. *et al.* Failure of blood-island formation and vasculogenesis in *Flk-1*-deficient mice. *Nature* **376**, 62–66 (1995).
16. Ashery-Padan, R., Marquardt, T., Zhou, X. & Gruss, P. Pax6 activity in the lens primordium is required for lens formation and for correct placement of a single retina in the eye. *Genes Dev.* **14**, 2701–2711 (2000).
17. Maruyama, K. *et al.* Inflammation-induced lymphangiogenesis in the cornea arises from CD11b-positive macrophages. *J. Clin. Invest.* **115**, 2363–2372 (2005).
18. Jeltsch, M. *et al.* Vascular endothelial growth factor (Vegf)/VEGF-C mosaic molecules reveal specificity determinants and feature novel receptor binding patterns. *J. Biol. Chem.* **281**, 12187–12195 (2006).
19. Baldwin, M.E. *et al.* The specificity of receptor binding by vascular endothelial growth factor-d is different in mouse and man. *J. Biol. Chem.* **276**, 19166–19171 (2001).
20. Streilein, J.W., Bradley, D., Sano, Y. & Sonoda, Y. Immunosuppressive properties of tissues obtained from eyes with experimentally manipulated corneas. *Invest. Ophthalmol. Vis. Sci.* **37**, 413–424 (1996).
21. Kirkin, V. *et al.* Characterization of indolinones which preferentially inhibit VEGF-C- and VEGF-D-induced activation of VEGFR-3 rather than VEGFR-2. *Eur. J. Biochem.* **268**, 5530–5540 (2001).
22. Cursiefen, C., Chen, L., Dana, M.R. & Streilein, J.W. Corneal lymphangiogenesis: evidence, mechanisms and implications for corneal transplant immunology. *Cornea* **22**, 273–281 (2003).
23. Liu, Y., Hamrah, P., Zhang, Q., Taylor, A.W. & Dana, M.R. Draining lymph nodes of corneal transplant hosts exhibit evidence for donor major histocompatibility complex (MHC) class II-positive dendritic cells derived from MHC class II-negative grafts. *J. Exp. Med.* **195**, 259–268 (2002).
24. Yamagami, S. & Dana, M.R. The critical role of lymph nodes in corneal alloimmunization and graft rejection. *Invest. Ophthalmol. Vis. Sci.* **42**, 1293–1298 (2001).
25. Chen, L. *et al.* Vascular endothelial growth factor receptor-3 mediates induction of corneal alloimmunity. *Nat. Med.* **10**, 813–815 (2004).
26. Yoon, Y.S. *et al.* VEGF-C gene therapy augments postnatal lymphangiogenesis and ameliorates secondary lymphedema. *J. Clin. Invest.* **111**, 717–725 (2003).
27. Mäkinen, T. *et al.* Inhibition of lymphangiogenesis with resulting lymphedema in transgenic mice expressing soluble *Vegf* receptor-3. *Nat. Med.* **7**, 199–205 (2001).
28. Karpanen, T. *et al.* Lymphangiogenic growth factor responsiveness is modulated by postnatal lymphatic vessel maturation. *Am. J. Pathol.* **169**, 708–718 (2006).
29. Cao, Y. *et al.* Vascular endothelial growth factor C induces angiogenesis *in vivo*. *Proc. Natl. Acad. Sci. USA* **95**, 14389–14394 (1998).
30. Kubo, H. *et al.* Blockade of vascular endothelial growth factor receptor-3 signaling inhibits fibroblast growth factor-2-induced lymphangiogenesis in mouse cornea. *Proc. Natl. Acad. Sci. USA* **99**, 8868–8873 (2002).
31. Cao, R. *et al.* Comparative evaluation of FGF-2-, VEGF-A- and VEGF-C-induced angiogenesis, lymphangiogenesis, vascular fenestrations and permeability. *Circ. Res.* **94**, 664–670 (2004).
32. Cursiefen, C. *et al.* VEGF-A stimulates lymphangiogenesis and hemangiogenesis in inflammatory neovascularization via macrophage recruitment. *J. Clin. Invest.* **113**, 1040–1050 (2004).
33. Cursiefen, C. *et al.* Lymphatic vessels in vascularized human corneas: immunohistochemical investigation using LYVE-1 and podoplanin. *Invest. Ophthalmol. Vis. Sci.* **43**, 2127–2135 (2002).
34. Hamrah, P. *et al.* Expression of vascular endothelial growth factor receptor-3 (VEGFR-3) on monocytic bone marrow-derived cells in the conjunctiva. *Exp. Eye Res.* **79**, 553–561 (2004).
35. Joukov, V. *et al.* Proteolytic processing regulates receptor specificity and activity of VEGF-C. *EMBO J.* **16**, 3898–3911 (1997).
36. Bernatchez, P.N., Rollin, S., Soker, S. & Sirois, M.G. Relative effects of VEGF-A and VEGF-C on endothelial cell proliferation, migration and PAF synthesis: role of neuropilin-1. *J. Cell. Biochem.* **85**, 629–639 (2002).
37. Roeckl, W. *et al.* Differential binding characteristics and cellular inhibition by soluble *Vegf* receptors 1 and 2. *Exp. Cell Res.* **241**, 161–170 (1998).
38. Fuh, G., Li, B., Crowley, C., Cunningham, B. & Wells, J.A. Requirements for binding and signaling of the kinase domain receptor for vascular endothelial growth factor. *J. Biol. Chem.* **273**, 11197–11204 (1998).
39. Wiesmann, C. *et al.* Crystal structure at 1.7 Å resolution of *Vegf* in complex with domain 2 of the Flt-1 receptor. *Cell* **91**, 695–704 (1997).
40. Goldman, J., Le, T.X., Skobe, M. & Swartz, M.A. Overexpression of VEGF-C causes transient lymphatic hyperplasia but not increased lymphangiogenesis in regenerating skin. *Circ. Res.* **96**, 1193–1199 (2005).
41. Vasioukhin, V., Degenstein, L., Wise, B. & Fuchs, E. The magical touch: genome targeting in epidermal stem cells induced by tamoxifen application to mouse skin. *Proc. Natl. Acad. Sci. USA* **96**, 8551–8556 (1999).
42. Ebos, J.M. *et al.* A naturally occurring soluble form of vascular endothelial growth factor receptor 2 detected in mouse and human plasma. *Mol. Cancer Res.* **2**, 315–326 (2004).
43. Ebos, J.M. *et al.* Vascular endothelial growth factor-mediated decrease in plasma soluble vascular endothelial growth factor receptor-2 levels as a surrogate biomarker for tumor growth. *Cancer Res.* **68**, 521–529 (2008).
44. Ebos, J.M., Lee, C.R., Christensen, J.G., Mutsaers, A.J. & Kerbel, R.S. Multiple circulating proangiogenic factors induced by sunitinib malate are tumor-independent and correlate with antitumor efficacy. *Proc. Natl. Acad. Sci. USA* **104**, 17069–17074 (2007).
45. Kaipainen, A. *et al.* Expression of the *fms*-like tyrosine kinase 4 gene becomes restricted to lymphatic endothelium during development. *Proc. Natl. Acad. Sci. USA* **92**, 3566–3570 (1995).
46. Huang, H.Y., Ho, C.C., Huang, P.H. & Hsu, S.M. Co-expression of VEGF-C and its receptors, VEGFR-2 and VEGFR-3, in endothelial cells of lymphangioma. Implication in autocrine or paracrine regulation of lymphangioma. *Lab. Invest.* **81**, 1729–1734 (2001).
47. Norgall, S. *et al.* Elevated expression of VEGFR-3 in lymphatic endothelial cells from lymphangiomas. *BMC Cancer* **7**, 105 (2007).
48. Wilting, J. *et al.* Embryonic development and malformation of lymphatic vessels. *Novartis Found. Symp.* **283**, 220–227; discussion 227–229, 238–241 (2007).
49. Azar, D.T. Corneal angiogenic privilege: angiogenic and antiangiogenic factors in corneal avascularity, vasculogenesis, and wound healing (an American Ophthalmological Society thesis). *Trans. Am. Ophthalmol. Soc.* **104**, 264–302 (2006).
50. Kerjaschki, D. *et al.* Lymphatic endothelial progenitor cells contribute to de novo lymphangiogenesis in human renal transplants. *Nat. Med.* **12**, 230–234 (2006).
51. Brideau, G. *et al.* Endostatin overexpression inhibits lymphangiogenesis and lymph node metastasis in mice. *Cancer Res.* **67**, 11528–11535 (2007).
52. Kojima, T., Azar, D.T. & Chang, J.H. Neostatin-7 regulates bFGF-induced corneal lymphangiogenesis. *FEBS Lett.* **582**, 2515–2520 (2008).
53. Bielenberg, D.R. *et al.* Semaphorin 3F, a chemorepellent for endothelial cells, induces a poorly vascularized, encapsulated, nonmetastatic tumor phenotype. *J. Clin. Invest.* **114**, 1260–1271 (2004).
54. Oka, M. *et al.* Inhibition of endogenous TGF-beta signaling enhances lymphangiogenesis. *Blood* **111**, 4571–4579 (2008).
55. Skobe, M. *et al.* Induction of tumor lymphangiogenesis by VEGF-C promotes breast cancer metastasis. *Nat. Med.* **7**, 192–198 (2001).
56. Mandriota, S.J. *et al.* Vascular endothelial growth factor-C-mediated lymphangiogenesis promotes tumour metastasis. *EMBO J.* **20**, 672–682 (2001).
57. Brakenhielm, E. *et al.* Modulating metastasis by a lymphangiogenic switch in prostate cancer. *Int. J. Cancer* **121**, 2153–2161 (2007).
58. He, Y. *et al.* Suppression of tumor lymphangiogenesis and lymph node metastasis by blocking vascular endothelial growth factor receptor 3 signaling. *J. Natl. Cancer Inst.* **94**, 819–825 (2002).
59. Hirakawa, S. *et al.* VEGF-C-induced lymphangiogenesis in sentinel lymph nodes promotes tumor metastasis to distant sites. *Blood* **109**, 1010–1017 (2007).

## ONLINE METHODS

**Mice.** We purchased BALB/c, C57BL/6J and K14Cre mice from the Jackson Laboratory. We generated *Vegfr2<sup>loxP/loxP</sup>* mice as described in the **Supplementary Methods**. LeCre mice<sup>16</sup> constitutively express Cre recombinase in the cornea. For all procedures, we anesthetized the mice by intraperitoneal injection of 50 mg per kg body weight ketamine hydrochloride (Fort Dodge Animal Health, Wyeth) and 10 mg per kg body weight xylazine (Phoenix Scientific). All mouse procedures were approved by the Animal Care and Use Committees at the University of Kentucky or Yokohama City University and conformed to the Association for Research in Vision and Ophthalmology Statement on Animal Research.

**Conditional *Vegfr2* gene ablation.** We achieved embryonic conditional genetic ablation of *Vegfr2* in the cornea by cross-breeding *Vegfr2<sup>loxP/loxP</sup>* mice with LeCre mice<sup>16</sup>. Alternatively, to target *Vegfr2* in the adult mouse cornea, we performed intrastromal injections of plasmids<sup>11</sup> containing the sequence for Cre recombinase driven by a cytomegalovirus promoter (pCre; 20  $\mu$ g) into one eye and an empty plasmid (pNull; 20  $\mu$ g) into the contralateral eye of *Vegfr2<sup>loxP/loxP</sup>* or BALB/c mice 3 d before suture placement. To achieve embryonic conditional genetic ablation of *Vegfr2* in the epidermis, we cross-bred *Vegfr2<sup>loxP/loxP</sup>* mice with K14Cre mice that constitutively express Cre recombinase in the skin epidermis and hair follicle<sup>41</sup>.

**Transmission electron microscopy.** We enucleated eyes from wild-type and LeCre;*Vegfr2<sup>loxP/loxP</sup>* mice and fixed them in 3.5% glutaraldehyde and 4% paraformaldehyde for 2 h followed by preparation of uranyl acetate- and lead citrate-stained ultrathin sections for transmission electron microscopy studies (Phillips Biotwin).

**Corneal injury.** We placed two intrastromal 11-0 sutures (Mani) in the mouse cornea 180° from each other. We placed all sutures in the midpoint between the limbus and the corneal apex and left them in place for up to 14 d. We injected plasmids coding for Cre and mouse sVegfr-2 (psVegfr-2) for *in vivo* enforced expression studies as shown previously<sup>11</sup>. To block Vegfr-3 activity, we performed daily intraperitoneal injections of the Vegfr-3 tyrosine kinase inhibitor (MAZ51, EMD Chemicals, 8 mg per kg body weight) in pCre-treated *Vegfr2<sup>loxP/loxP</sup>* mice after corneal suture placement for 14 consecutive d. We administered vehicle only (DMSO) as a control treatment.

**Vegf-C neutralization.** We performed intrastromal injections of rabbit neutralizing antibody to Vegf-c (Angio-Proteomie, pV1006R-r, 16  $\mu$ g) into one eye and control rabbit IgG (16  $\mu$ g) into the contralateral eye on the day of suture placement and every 3 d thereafter for 14 d.

**VEGFR-2 phosphorylation assay.** We cultured porcine aortic endothelial cells stably transfected with VEGFR-2 (PAE-KDR cells, Sibtech) in DMEM (Invitrogen) containing 10% FBS, penicillin G (100 U ml<sup>-1</sup>), streptomycin sulfate (0.1 mg ml<sup>-1</sup>) (all from Sigma Aldrich) at 37 °C, 10% CO<sub>2</sub> and 90% room air. Upon attaining 80% confluence, we serum-starved these cells for 24 h, after which time we exposed them to VEGF-A (R&D Systems, 2.5 nM) or medium alone (negative control) and monomeric sVEGFR-1 (Reliatech, 15 nM), monomeric sVEGFR-2 (Reliatech, 75 nM), dimeric VEGFR2-Fc (R&D Systems, 75 nM) or IgG-Fc control (Jackson ImmunoResearch, 75 nM) for 15 min. We processed the lysates in RIPA buffer (Sigma-Aldrich), resolved the proteins by 8% SDS-PAGE and transferred them to nitrocellulose membranes. We performed immunoblotting with a rabbit antibody specific for phosphorylated VEGFR-2 (1 in 500, Upstate, 36-019), and we assessed loading with antibodies specific for VEGFR-2 (1 in 1,000, R&D Systems, AF357) and Vinculin (1 in 2,000, Sigma, V4139).

**Silver staining.** We resolved VEGFR-2-Fc or sVEGFR-2 by 10% SDS-PAGE and stained the gels with SilverSNAP Stain (Pierce) according to the manufacturer's instructions.

**Immunomorphometric analyses.** We performed immunostaining and flat mounting as previously shown<sup>11</sup> with rabbit antibody specific for mouse Lyve-1 (Abcam; 1 in 333), rat antibody specific for mouse CD31 (BD Biosciences; 1 in 50), rat antibody specific for mouse MECA-32 (BD Biosciences; 1 in 10),

goat antibody specific for mouse Lyve-1 (R&D Systems, 1 in 100) and rabbit antibody specific for mouse Prox-1 (Angiobio; 1 in 500) for 48 h at 4 °C. We used Alexa Fluor 488-labeled goat antibody to rabbit IgG (1 in 200) and donkey antibody to goat IgG (1 in 200, Invitrogen), or Cy3-conjugated donkey antibody to rabbit IgG (Jackson ImmunoResearch; 1 in 400) for 24 h as secondary antibodies. We visualized tissue mounts under fluorescent microscopy (Leica SP-5) and analyzed the images with ImageJ software (US National Institutes of Health). We calculated the mean percentage Lyve-1<sup>+</sup> (lymphatic vessel) or CD31<sup>+</sup>Lyve-1<sup>-</sup> (blood vessel) areas for corneal flat mounts and skin whole mounts with ImageJ software. We counted the number of Prox1<sup>+</sup> nuclei within Lyve-1<sup>+</sup> skin lymphatic vessels in 12 random fields and expressed it as LEC density per 100  $\mu$ m. We determined the density of lymphatic structures by counting lymphatic vessel branch points per unit area (750  $\mu$ m  $\times$  750  $\mu$ m) on standard low-magnification Lyve-1-stained images of the mouse skin.

**Mouse endothelial cell culture.** We cultured mouse blood endothelial cells from brain (Bend3), pancreas (MS1) and skin (Py4) and LECs from mesenteric adventitial tissue<sup>60</sup> in DMEM (Invitrogen) containing 10% FBS, penicillin G (100 U ml<sup>-1</sup>) and streptomycin sulfate (0.1 mg ml<sup>-1</sup>) (all from Sigma Aldrich) at 37 °C, 10% CO<sub>2</sub> and 90% room air. Upon attaining 80% confluence, we serum-starved these cells for 24 h, after which we collected supernatant fractions for sVegfr-2 protein quantification by ELISA. We also extracted total RNA for RT-PCR.

**Human lymphatic microvascular endothelial cell proliferation assay.** We maintained cultured human lymphatic microvascular endothelial cells (Cambrex) in EGM-2 MV medium (Clonetics) supplemented with 10% FBS and antibiotics at 37 °C under 5% CO<sub>2</sub> and 95% room air. We plated confluent cells in a 96-well plate at a density of 30,000 cells per well. We serum-starved the cells for 2 h and then exposed them to medium alone (MCDB 131 + 5% FBS), VEGF-C (200 ng ml<sup>-1</sup>; R&D Systems)-enriched medium or VEGF-C-enriched medium with sVEGFR-2 (13.6  $\mu$ g ml<sup>-1</sup>). This concentration of sVEGFR-2 corresponds to a molar ratio of approximately 11:1 compared to VEGF-C and therefore represents a physiological concentration in view of our finding that sVegfr-2 levels in mouse cornea are ~20-fold higher than Vegf-c levels on a molar basis. We quantified proliferation by BrdU uptake (Chemicon International) at 36 h after incubation with VEGF-C.

**Lymphangioma proliferation assay.** We isolated lymphatic endothelial cells from lymphangiomas from two individuals, 4 and 10 months of age<sup>47</sup>, with the approval of the Ethics Committee of the Georg-August-University and with the informed consent of the subjects' parents. We grew these cells in EGM2-MV growth medium containing 5% FBS. We passaged the cells onto a 96-well plate (5,000 cells per well) in basal medium (MCDB131) containing 2% FBS and allowed them to adhere overnight. We then treated the cultures with 200 ng ml<sup>-1</sup> recombinant human wild-type VEGF-C (Reliatech) alone or together with 25  $\mu$ g ml<sup>-1</sup> of sVEGFR-2 (Reliatech) in basal medium with 0.1% FBS. We measured cell proliferation after 24 h by using the BrdU cell proliferation kit (Chemicon) according to the manufacturer's instructions.

**Western blotting.** We resolved mouse cornea lysates as well as cell culture supernatants by 8% SDS-PAGE or 4–20% PAGE and transferred the proteins to nitrocellulose membranes. We then immunoblotted with a rabbit antibody against the amino terminus of mouse Vegfr-2 (1 in 1,000; clone T014; ref. 12) or custom-made sVegfr-2-specific antibody (1 in 1,000; AA21127) and assessed loading with rabbit antibody against human GAPDH (1 in 2,000; Abcam).

**Immunoprecipitation studies.** We incubated recombinant mouse sVegfr-2 (2  $\mu$ g) with mouse recombinant Vegf-C (100 ng, Biovision) in PBS at 4 °C for 1 h. We carried out immunoprecipitation with 2  $\mu$ g of a Vegfr-2-specific antibody or an isotype control IgG. We used immobilized protein A/G beads (20  $\mu$ l, Pierce) for precipitation. We boiled samples, resolved them by SDS-PAGE with appropriate positive controls (recombinant sVegfr-2 and Vegf-c) and transferred them to a nitrocellulose membrane. We used rabbit antibodies specific for Vegf-c (1 in 1,000, Santa Cruz) and Vegfr-2 (1 in 1,000, T014) to probe for Vegf-c and Vegfr-2, respectively. We performed immunoprecipitation of Vegfr-2 from mouse plasma as described previously<sup>42</sup>. We used rabbit antibody against Vegfr-2 (T014, 2  $\mu$ g) for immunoprecipitation. We used T014 (1:1000), goat antibody

to the C-terminus of Vegfr-2 (1 in 1,000, Abcam-ab2349) or rabbit antibody to sVegfr-2 (1 in 1,000, AA21127) for immunoblotting. We incubated mouse LECs with medium only or Vegf-c (200 ng ml<sup>-1</sup>, Biovision) with or without sVegfr-2 (13.8 µg ml<sup>-1</sup>) or Vegfr-1-Fc (20 µg ml<sup>-1</sup>, R&D Systems) for 15 min. We used equimolar concentrations of sVegfr-2 and Vegfr-1-Fc. We immunoprecipitated the lysates with Vegfr-3-specific antibody (Santa Cruz, C-20), immunoblotted with antibody to phosphotyrosine (Millipore, 4G10, 1 in 1,000) and reblotted with Vegfr-3-specific antibody (eBioscience, AFL4, 1:500).

**Statistical analyses.** We used the Mann-Whitney *U* test with Bonferroni correction for statistical comparison of multiple variables. We determined corneal transplant survival by Kaplan-Meier survival. The null hypothesis was rejected at  $P < 0.05$ .

**Additional methods.** Detailed methodology is described in the **Supplementary Methods**.

60. Ando, T. *et al.* Isolation and characterization of a novel mouse lymphatic endothelial cell line: SV-LEC. *Lymphat. Res. Biol.* **3**, 105–115 (2005).